Ray-optical refraction with confocal lenslet arrays

2008 New J. Phys. 10 083033

(http://iopscience.iop.org/1367-2630/10/8/083033)

New Journal of Physics
The open-access journal for physics

Ray-optical refraction with confocal lenslet arrays

Johannes Courtial
Department of Physics and Astronomy, University of Glasgow, Glasgow G12 8QQ, UK
E-mail: j.courtial@physics.gla.ac.uk

New Journal of Physics **10** (2008) 083033 (8pp)
Received 27 May 2008
Published 22 August 2008
Online at http://www.njp.org/
doi:10.1088/1367-2630/10/8/083033

Abstract. Two parallel lenslet arrays with focal lengths f_1 and f_2 that share a common focal plane (that is, which are separated by a distance $f_1 + f_2$) can refract transmitted light rays according to Snell's law, but with the 'sin's replaced with 'tan's. This is the case for a limited range of input angles and other conditions. Such confocal lenslet arrays can therefore simulate the interface between optical media with different refractive indices, n_1 and n_2, whereby the ratio $\eta = -f_2/f_1$ plays the role of the refractive-index ratio n_2/n_1. Suitable choices of focal lengths enable positive and negative refraction. In contrast to Snell's law, which leads to nontrivial geometric imaging by a planar refractive-index interface only for the special case of $n_1 = \pm n_2$, the modified refraction law leads to geometric imaging by planar confocal lenslet arrays for any value of η. We illustrate some of the properties of confocal lenslet arrays with images rendered using ray-tracing software.

Contents

1. Introduction

In 1908, Lippmann suggested a method for three-dimensional (3D), 'integral', photography [1]. A scene is imaged onto the film not with a single lens but with a lenslet array, whereby each lenslet creates a small image of the whole scene as seen from its position. When suitably developed and viewed through a similar lenslet array, the integral photo displays 3D information of the photographed scene. This idea forms the basis of many 3D displays [2]. If the lenslet array used for viewing is rotated relative to the photo, a Moiré magnifier results [3]. In a simplified form—using cylindrical lenses instead of spherical lenses—this idea is also the basis of lenticular printing, the technique used to create 3D postcards that provide two or more different images when seen from different positions [4].

Lippmann also suggested a combination of two lenslet arrays that are separated by the sum of their focal distances, that is, the two lenslet arrays are confocal. The lenslets in the first array create images of a scene as seen from their position. From these images, the lenslets in the second array create a 3D, pseudoscopic (that is, depth-inverted) image of the scene [5] (or, in the case of the Moiré magnifier, a scaled image [3]). Confocal lenslet arrays have recently been realized in impressive quality and scale [6].

The inversion of the transverse ray direction in Lippmann's confocal lenslet arrays discussed above is equivalent to the inversion of the angle of the ray with respect to the surface normal that happens on reversal of the refractive index. Ray-optically, the confocal lenslet arrays discussed above therefore act like the planar interface between two materials, one with refractive index $+n$, the other with refractive index $-n$. (This is also true for combinations of arrays of miniaturized Dove prisms [7].) What is interesting about the realization that confocal lenslet arrays have the effect of negative refraction is that the now burgeoning field of metamaterials also started off with negative refraction: by building materials consisting of resonant structures smaller than the wavelength, it was first possible to achieve a negative refractive index [8, 9]. The field then moved in exciting directions, for example, the development of new optical-design paradigms that use the new-found freedom to give materials arbitrary refractive indices, and vary these across the material. One of the aims of this paper is to start the process of developing lenslet arrays in a similar way.

This paper is organized as follows. Section 2 derives the formal similarity between the ray-optics of confocal lenslet arrays and refractive-index changes. Section 3 considers the imaging properties of confocal lenslet arrays. Section 4 presents images rendered using ray-tracing software to illustrate the basic optical properties of confocal lenslet arrays. Finally, section 5 concludes.

2. Confocal lenslet arrays and Snell's law

This section derives a law, similar to Snell's law, that describes the change in the direction of light rays transmitted through confocal lenslet arrays.

Figure 1(a) shows two lenses with focal lengths f_1 and f_2, centred on the same optic axis, which are separated by their focal lengths, $f_1 + f_2$. Light rays hitting the left lens at an angle α_1 with respect to the optic axis pass through the common focal plane a distance $\tan\alpha_1 = y/f_1$. Provided they then pass through the corresponding lens on the right (which can be aided by appropriately redirecting the rays in the focal plane, for example, with a field lens or a scatterer), such rays leave at an angle α_2 with respect to the optic axis such that $\tan\alpha_2 = -y/f_2$.

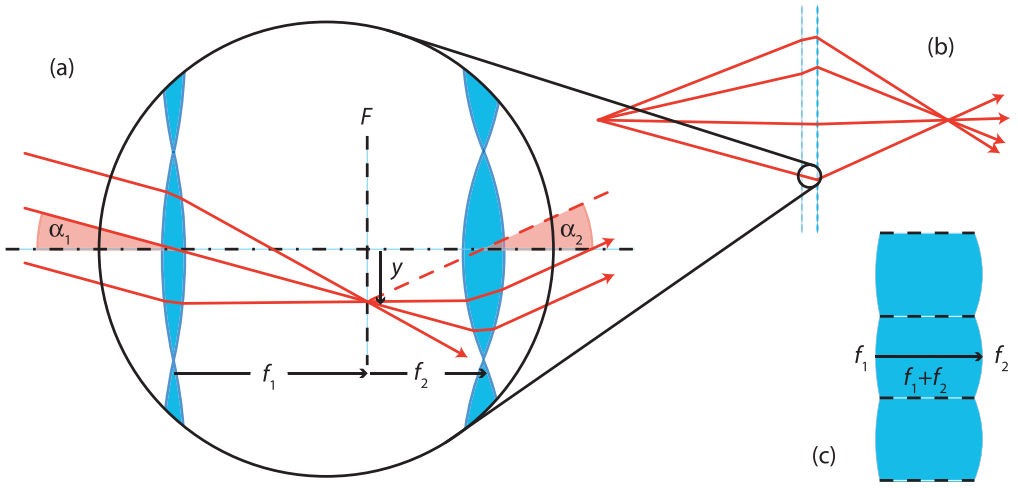

Figure 1. Ray-optics of confocal lenslet arrays. (a) An individual lens (focal length f_1) in the left lenslet array focuses all incident light rays with the same angle of incidence α_1 to a point in the focal plane F. These rays leave the corresponding lens (focal length f_2) in the right array with an exit angle α_2, such that $f_1 \tan\alpha_1 = -f_2 \tan\alpha_2$. (b) The confocal lenslet arrays have the imaging properties of the interface between two media with different refractive indices. In the example shown here, one of the refractive indices is positive, the other negative. (c) Confocal lenslet arrays can be manufactured from a single sheet of material, whereby each surface acts like a single lenslet array. Each surface is covered in spherical bumps, each of which acts as a lenslet. The radius of curvature of the bumps has to be $r_{1,2} = f_{1,2}(n-1)/n$, where n is the refractive index of the sheet material, to focus parallel light rays a distance $f_{1,2}$ inside the material. Stray light, that is light that would not pass through corresponding lenslets, can in principle be absorbed by an absorber sheet (dashed lines) separating neighbouring pairs of corresponding lenslets.

Eliminating y from these equations gives

$$f_1 \tan\alpha_1 = -f_2 \tan\alpha_2. \tag{1}$$

The two lenses are now part of two confocal lenslet arrays (figure 1(b)). Equation (1) still holds, but now α_1 and α_2 are the angles of incidence and exit with respect to the surface normal, that is the normal to the plane of the lenslet arrays. Comparison with Snell's law of refraction,

$$n_1 \sin\alpha_1 = n_2 \sin\alpha_2, \tag{2}$$

reveals that, for small angles $\alpha_{1,2}$, when the approximations $\tan\alpha_{1,2} \approx \sin\alpha_{1,2} \approx \alpha_{1,2}$ hold, the equations governing the change of ray direction in confocal lenslet arrays and Snell's law are the same. The quantity

$$\eta = -\frac{f_2}{f_1} \tag{3}$$

plays the role of the ratio of the refractive indices, that is

$$\eta = -\frac{f_2}{f_1} \approx \frac{n_2}{n_1}. \tag{4}$$

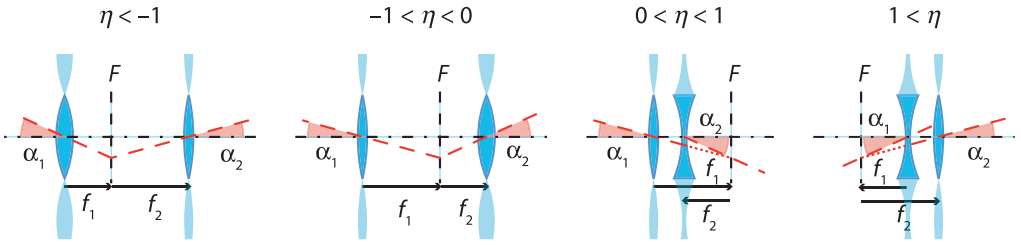

Figure 2. Realization of different values of η with confocal lenslet arrays. Values of $\eta < 0$ and $\eta > 0$ can, respectively, be realized with two convex ($f > 0$; left) lenses and a combination of a convex and a concave ($f < 0$; right) lens. In each case, one pair of corresponding lenslets is shown together with the common focal plane, F, and light rays travelling from left to right (incidence angle α_1, exit angle α_2) that pass through the centre of one lens and which intersect (real or virtual) in the focal plane. (In the case of virtual intersections, dotted lines indicate the continuation of the relevant light rays.)

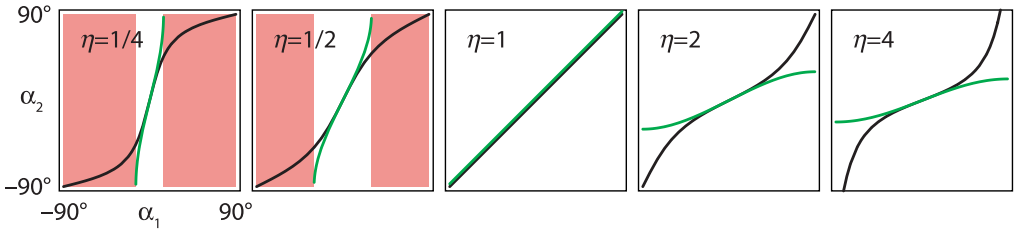

Figure 3. Refraction (green curves) compared with refraction simulated with confocal lenslet arrays (black curves). $\alpha_2(\alpha_1)$ calculated according to equation (2) (green lines) and equation (1) with $-f_2/f_1 = \eta$ (black lines). The curves agree for small angles, but, for $|\eta| \neq 1$, disagree for larger angles. This is particularly apparent for values of α_1 for which Snell's law predicts total internal reflection (TIR) (red shaded areas). Both α_1 and α_2 are plotted over the range -90° to 90°. A number of η values are shown. All η values are positive; for the corresponding negative values, α_2 changes sign.

The fact that a confocal lenslet array can act similar to a refractive-index interface is the key result of this paper.

Figure 2 shows that, in principle, any refractive-index ratio can be approximated by confocal lenslet arrays. In particular, it shows how positive values of η can be realized using a combination of two lenslet arrays with different focal lengths, one positive, the other negative.

Figure 3 plots the dependence of the angle of refraction on the angle of incidence, both for refraction at refractive-index changes, that is refraction described by Snell's law (equation (2)), and for refraction at confocal lenslet arrays (equation (1)). For small angles, the two are very similar, as expected. For large angles, however, there are significant deviations. Perhaps most strikingly, in confocal-lenslet-arrays refraction both the angle of incidence and the angle of refraction range from -90° to $+90^\circ$ for all values of η. This is in contrast to Snell's-law refraction, where either the angle of incidence (in the case of refraction into the optically thinner medium, that is for $|n_1| > |n_2|$) or the angle of refraction (in the case of refraction into the

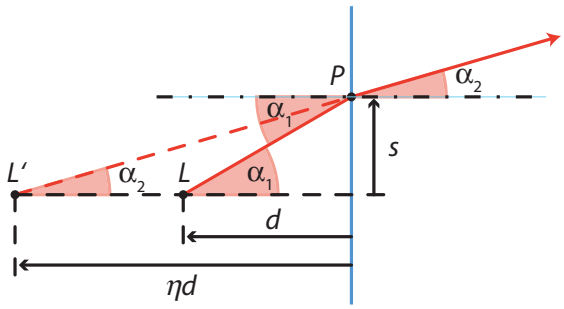

Figure 4. Geometry of longitudinal imaging due to refraction according to equation (1). A light ray (solid red line) from a point light source L hits a confocal lenslet arrays and is refracted there according to equation (1); the angles of incidence and refraction are α_1 and α_2; P is the point where the ray hits the confocal lenslet arrays (blue line). The continuation of the refracted ray (dashed red line) passes through the point L', the image of L. L and L' are located on the same normal to the confocal lenslet arrays. If the distance of L in front of the confocal lenslet arrays is called d, then the distance of L' in front of the confocal lenslet arrays is ηd. The figure is drawn for $\eta = 2$.

optically denser medium, $|n_1| < |n_2|$) are restricted to a smaller range of angles. This means that there is no equivalent of TIR in confocal-lenslet-array refraction.

The next section contrasts geometric imaging by a plane that refracts light rays according to equation (1) with a plane that refracts according to Snell's law.

3. Imaging properties of confocal lenslet arrays

Consider a point light source L a distance d in front of a confocal lenslet array with η (figure 4). In order for the point light source to be exactly imaged to a location L' a distance ηd in front of the arrays, the continuations of all light rays have to intersect at L'. As can be seen from figure 4, the angles of incidence and refraction, α_1 and α_2, have to satisfy the equations

$$\tan\alpha_1 = \frac{s}{d} \tag{5}$$

and

$$\tan\alpha_2 = \frac{s}{\eta d}, \tag{6}$$

which can be simplified to

$$\tan\alpha_1 = \eta \tan\alpha_2. \tag{7}$$

This is, of course, equation (1) with the definition (4).

This result is worth discussing. The change in apparent depth when looking into a medium with a different optical density, for example, looking from air into water, is well known. But it works exactly only for small angles, namely when the sines in Snell's law can be replaced by tangents. The deviations from geometric imaging can be seen directly: when seen through a planar water surface, a finger partially submerged in the water seems to bend when the viewing

position is changed. For confocal lenslet-array refraction, geometric imaging occurs which is, in principle, exact for all angles. This important property is illustrated in the following section.

4. Illustration of the optical properties of confocal lenslet arrays using ray tracing

Here, we use the freely-available rendering software POV-ray [10] to illustrate some of the properties of confocal lenslet arrays. Note that these illustrations are full computer simulations of light rays being refracted on passage through the detailed structure of a specific realization of confocal lenslet arrays.

Rendering based on ray tracing simulates a photo being taken of a virtual scene programmed into the computer. It works as follows. Physical light rays originate at a light source before reflecting, scattering or refracting off objects. When taking a photo of a scene, only those light rays that are deflected such that they pass through a camera's lens and hit the detector chip (or film) contribute to the photo. Rendering based on ray tracing considers only those light rays. Starting from the position of one of the virtual pixels of the virtual camera's detector chip, the light rays are geometrically traced *backwards* through the virtual camera lens, and to the virtual objects that make up the virtual scene. In the simplest case, such a light ray hits a coloured object; the pixel from which the light ray was traced backwards is then given the object's colour. Pixel-by-pixel, rendering software based on ray tracing traces light rays from all pixels in the virtual camera's virtual detector, thereby producing a complete image of the virtual scene. A more complete explanation of ray tracing can be found in [11].

We simulate here a specific realization of confocal lenslet arrays. Corresponding lenslets are spherical bumps at opposite ends of a single piece of glass (refractive index $n = 1.5$). A bump with a radius of curvature r on the surface of a material with refractive index n focuses a collimated light beam a distance f inside the material, whereby

$$f = \frac{n}{n-1} r; \tag{8}$$

negative focal lengths correspond to bumps with a negative radius of curvature, that is, 'bumps' that are actually dips. Therefore a piece of glass with a surface bump of radius r_1 at one end, and of radius r_2 on the other end, and of length $f_1 + f_2$, where the fs are related to the corresponding rs according to equation (8), acts like two confocal lenslets.

The confocal lenslet arrays formed from these pieces of glass are square arrays, so when viewed along the optic axis (which passes through the centre of both lenslets), each piece of glass has a square cross-section. Unless otherwise indicated, neighbouring pairs of corresponding lenslets are separated from each other by absorbers (figure 1(c)); this absorbs all light rays other than those that enter and exit through corresponding lenslets.

Figure 5 simulates the view through confocal lenslet arrays with various values of η. The apparent position of an object placed behind the arrays is that of an object placed inside a medium with refractive index n_1, seen from within a medium with refractive index n_2. The apparently closer position of the object in the case $\eta = 0.5$ corresponds to the apparent shortening of a leg dipped into a swimming pool when seen from above the water. The object's apparently more distant position in the cases $\eta = 2$ and 4 corresponds to the increased distance of objects above the pool when seen from underwater. The cases $\eta = -1$ and -0.5 cannot be observed in a swimming pool: they correspond to the boundary between refractive indices with opposite signs. In these cases, the object's apparent position is in front of the arrays, and its image is pseudoscopic, that is depth-inverted [12].

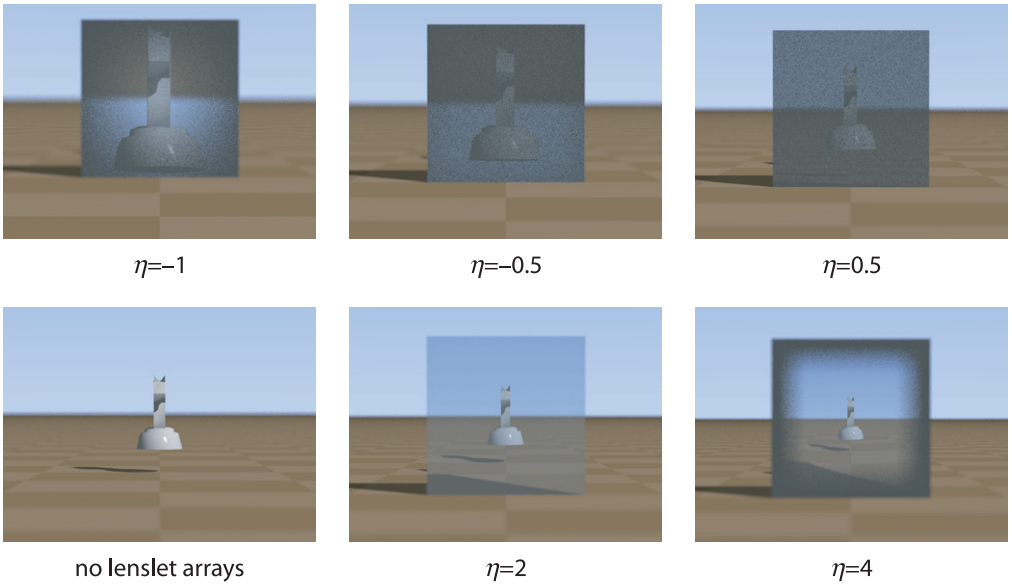

Figure 5. Looking through confocal lens arrays with different values of η. In the virtual scene rendered here, a chess piece is positioned behind two confocal lenslet arrays (200×200 lenslets). For comparison, the chess piece is also shown in the same position without the lenslet arrays. Light rays travelling from the chess piece to the camera would first encounter the back lenslet array of focal length f_1 and then the front lenslet array of focal length f_2. In the different frames, the focal lengths are chosen such that $\eta = -f_2/f_1$. The confocal lenslet arrays then act like the interface between a medium behind the arrays with refractive index n_1, and a medium in front of the arrays with refractive index n_2, where $\eta \approx n_2/n_1$. In units of side lengths of squares on the chequered floor, the distance between the camera and the lenslet arrays is 6, the distance between the lenslet arrays and the chess piece is 2, the area of the lenslet arrays is 1×1, and the focal lengths in the different frames are $f_1 = f_2 = 0.8$ ($\eta = -1$); $f_1 = 0.5$, $f_2 = 1$ ($\eta = -0.5$); $f_1 = -0.5$, $f_2 = 1$ ($\eta = 0.5$); $f_1 = 1$, $f_2 = -0.5$ ($\eta = 2$); $f_1 = 1.6$, $f_2 = -0.4$ ($\eta = 4$).

Figure 5 also illustrates a major limitation of confocal-lenslet-array refraction. Starting at the sheet's centre and moving outwards, the image appears to faint quite suddenly close to the edge in the frame calculated for $\eta = 4$; it starts to faint as soon as the centre is left in the $\eta = -1$ frame; and it is darkened everywhere in the frames $\eta = \pm 0.5$. This is due to the absorber between neighbouring lenslet pairs being visible from the camera position; in ray-tracing terms, rays that are traced backwards from the camera hit the absorber, so the corresponding pixel is black. An in-depth investigation of this limitation is outside the scope of this paper, but will be performed elsewhere [13].

5. Conclusions and future work

This paper introduces the concept of a sheet material that, with certain limitations, acts like the *interface* between two optical media with different—and, within certain limits,

arbitrary—refractive indices. In the sense that it leads to better 3D imaging, one of the limitations, namely deviations from Snell's law for larger angles of incidence and refraction, can be seen as an improvement on Snell's law. This should open up interesting imaging possibilities.

What makes this work particularly interesting is that the sheet material can act like the interface between media whose refractive indices have opposite signs. In this sense, this work is related to the current research interest in negative-refractive-index materials. Once realized experimentally, it will allow the strange optics of negative refraction to be 'experienced' on a macroscopic scale.

The ideas outlined here are the starting point for a much wider investigation of ray-engineering possibilities using lenslet arrays. Ideally, this will borrow concepts developed in the context of metamaterials, for example, the coordinate-transform optical design paradigm [14], which might be possible by utilizing additional design parameters such as the angle and displacement of individual lenslets (while keeping them confocal at all times). Most importantly, however, lenslet-array refraction has to be demonstrated experimentally.

Acknowledgments

Thanks to Ian Shanks for sharing his encyclopedic knowledge of 3D imaging and bringing to my attention much related earlier work. JC is a Royal Society University Research Fellow.

References

[1] Lippmann G 1908 La photographie intégrale *C. R. Séances Acad. Sci.* **146** 446–51
[2] Okoshi T 1980 Three-dimensional displays *Proc. IEEE* **68** 548–64
[3] Hutley M C, Hunt R, Stevens R F and Savander P 1994 The moiré magnifier *Pure Appl. Opt.* **3** 133–42
[4] Anderson K 1970 Lenticular device and method for providing same *US Patent* 3538632
[5] Ives H E 1931 Optical properties of a Lippman lenticulated sheet *J. Opt. Soc. Am.* **21** 171–6
[6] Stevens R F and Harvey T G 2002 Lens arrays for a three-dimensional imaging system *J. Opt. A: Pure Appl. Opt.* **4** S17–21
[7] Courtial J and Nelson J 2008 Ray-optical negative refraction and pseudoscopic imaging with Dove-prism arrays *New J. Phys.* **10** 023028
[8] Pendry J B, Holden A J, Robbins D J and Stewart W J 1998 Low frequency plasmons in thin-wire structures *J. Phys.: Condens. Matter* **10** 4785–809
[9] Pendry J B and Smith D R 2003 Reversing light: negative refraction *Phys. Today*
[10] 2006 POV-Ray—The Persistence of Vision Raytracer Online at http://www.povray.org/
[11] Wikipedia 2007 Ray tracing Online at http://en.wikipedia.org/wiki/Ray_tracing_(graphics) (Accessed 12/8/2008)
[12] Wade N J 2004 Philosophical instruments and toys: optical devices extending the art of seeing *J. Hist. Neurosci.* **13** 102–24
[13] Courtial J 2008 Ghost images and non-standard refraction with confocal lenslet arrays, in preparation
[14] Pendry J B, Schurig D and Smith D R 2006 Controlling electromagnetic fields *Science* **312** 1780–2